

Pareto Optimized EDCA Parameter Control for Wireless Local Area Networks

Minseok Kim¹, Wui Hwan Oh¹, Jong-Moon Chung¹, Bong Gyou Lee²,
Myunghwan Seo³, Jung-sik Kim³, and Hyung-Weon Cho³

¹School of Electrical & Electronic Engineering, Yonsei University, Seoul, Republic of Korea

²Graduate School of Information, Yonsei University, Seoul, Republic of Korea

³Samsung Thales Co., LTD., Seongnam-si, Gyeonggi-do, Republic of Korea

[e-mail: jmc@yonsei.ac.kr]

*Corresponding author: Jong-Moon Chung

Received May 8, 2014; revised October 2, 2014; accepted October 2, 2014; published October 31, 2014

Abstract

The performance of IEEE 802.11e enhanced distributed channel access (EDCA) is influenced by several interactive parameters that make quality of service (QoS) control complex and difficult. In EDCA, the most critical performance influencing parameters are the arbitration interframe space (AIFS) and contention window size (CW) of each access category (AC). The objective of this paper is to provide a scheme for parameter control such that the throughput per station as well as the overall system throughput of the network is maximized and controllable. For this purpose, a simple and accurate analytical model describing the throughput behavior of EDCA networks is presented in this paper. Based on this model, the paper further provides a scheme in which a Pareto optimal system configuration is obtained via an appropriate CW control for a given AIFS value, which is a different approach compared to relevant papers in the literature that deal with CW control only. The simulation results confirm the effectiveness of the proposed method which shows significant performance improvements compared to other existing algorithms.

Keywords: Enhanced distributed channel access, medium access control, parameter control, quality of service, wireless local area network

This research was supported by a grant-in-aid of Samsung Thales and the National IT Industry Promotion Agency (NIPA) Information Technology Research Center (ITRC) NIPA-2014-H0301-14-1015 and ICT R&D MSIP/IITP 13-911-05-002 (Access Network Control Techniques for Various IoT Services) program of the Ministry of Science, ICT and Future Planning (MSIP), Republic of Korea.

<http://dx.doi.org/10.3837/tiis.2014.10.010>

1. Introduction

Wireless local area networks (WLANs) are extensively deployed at various locations serving a wide variety of services and applications. The IEEE 802.11e standard provides enhancements in supporting service differentiations and Quality of Service (QoS) for WLANs [1]. The core scheme for service differentiation in IEEE 802.11e is the enhanced distributed channel access (EDCA). EDCA introduces four kinds of access categories (ACs) in which service differentiation is accomplished by applying different QoS parameters to each AC. These parameters include the contention window (CW) size and arbitration interframe space (AIFS) of each AC. ACs with higher priority are assigned smaller CW and AIFS values to result in a higher probability of channel access. However, the default parameter recommendations in [1] do not enable an optimal performance. In addition, there is no QoS provisioning mechanism that can be used as a reference to control the throughput of the individual ACs while maximizing the overall throughput of the WLAN.

Considering EDCA parameter control, a closed form solution for CW control to achieve weighted max-min fairness is proposed in [2]. The proposed scheme of [2] does not provide user controllability to allocate resources per AC. Similarly, [3] proposed CW adaptation methods based on the estimated network conditions, while [4] extended this model to consider delay requirements. On the other hand, user controllability on a throughput ratio allocated to each AC is provided in [5-6], but these papers do not consider maximization of system throughput simultaneously. These two issues are jointly considered in [7].

All of the relevant papers mentioned above deal with CW control only, and assume all of the stations operate with the same AIFS values. A reason for this is because of its simplicity and in [2], it is proven that for a single-hop network, the best average performance (in terms of overall system throughput) is obtained when all AIFSs are set the same. However, AIFS is a critical performance influencing parameter as shown in [8-12] and neighboring devices using EDCA commonly do not coordinate all ACs to have the same AIFSs among different devices. Therefore, naturally, devices with different AIFS settings will exist in the same region. In addition, for multi-hop networks, there exists a severe starvation problem even for very simple network topologies [13]. In these cases, not only the CW but the AIFS can be very useful in enhancing and controlling the performance of a network.

From the above-mentioned observations, in this paper, we focus on a mechanism that provides an optimal system performance while maintaining the desired ratio of throughput allocated to each AC, and thus, to enable user controllability. For this purpose, a simple and accurate analytical model describing the throughput behavior of EDCA networks is presented, and based on this a scheme that provides Pareto optimal system configuration is introduced, in which the CW of each station is appropriately adjusted for a given AIFS. The throughput performance of a station is in conflict of interest with the other stations, and therefore, a slight change in system parameters of one station to enhance its performance will eventually result in degradations on the performance of the other stations. Due to these parameters being highly interactive and correlated, multi-objective Pareto optimization is applied. In addition, the proposed scheme enables user controllability of the essential QoS parameters.

The remainder of the paper is organized as follows. Section II describes the saturation throughput model and also presents the problem statement that will be optimized. Section III introduces the proposed QoS provisioning algorithm, followed by the simulation results in section IV and the conclusion in section V.

2. System Model

Several models have been proposed for performance evaluation of EDCA networks [2], [5-6], [9-12]. Based on the Markov chain (M_1) modeling of the behavior of EDCA backoff procedures, the conditional collision probability (p_i) and the probability that a station of AC[i] transmits (τ_i) are computed and used to obtain the throughput performance. To compute the conditional collision probability p_i , most of the relevant works rely on a zone-based approach which require an additional Markov chain (M_2) [10-12]. In this model, the total influences that a station experiences in a specific contention zone are computed. The overall collision probability is averaged after computing all of the zone-specific probabilities. As a result, the complexity of the model increases significantly when there are multiple ACs and multiple contention-zones (almost impossible to be expressed in closed-forms). For this reason, the models in [10-12] can capture only two ACs with the same number of stations per AC.

Considering the above observations, the model introduced in this paper does not rely on contention-zones. Instead, the influences of various AIFS differences are incorporated in the Markov chain M_1 and does not require M_2 , which reduces the complexity of the model significantly (any number of ACs can be supported with a different number of stations per AC). In addition, a unified view of channel states is incorporated instead of the individual zone-specific view of channel states. A comparison between the previous models and the model introduced in this paper is depicted in Fig. 1.

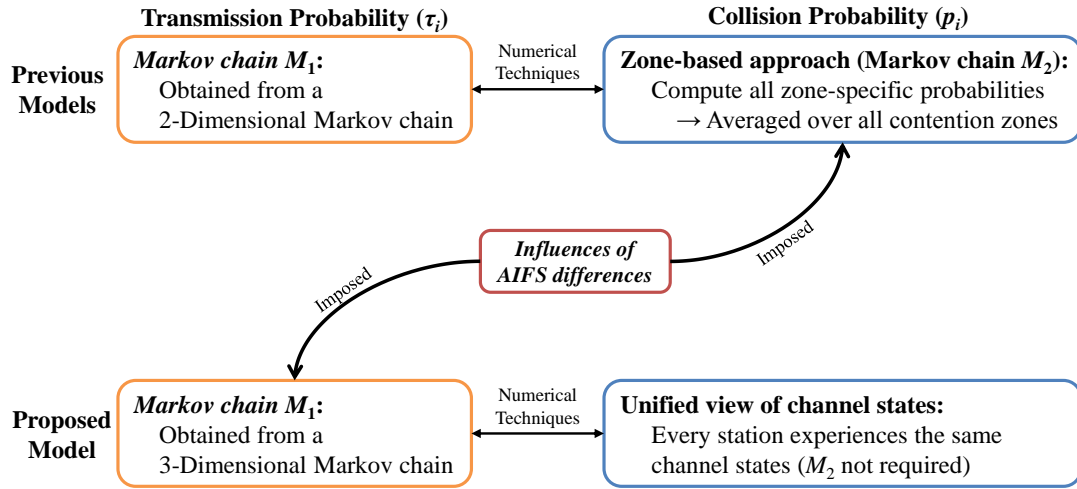


Fig. 1. Comparison between models.

The following assumptions and notations are used to set up the model. First, the saturation condition is assumed, meaning that each station always have packets to transmit. Secondly, any station that occupies the channel will transmit within a fixed size duration. These assumptions are widely adopted by most of the relevant papers in the literature [2-14]. It is assumed that there are M number of ACs in the network and X_i is the set of all stations that belongs to AC[i]. The number of stations in AC[i] is denoted as N_i (i.e., $N_i = |X_i|$). In addition, the set of all stations in the network is denoted as X and the total number of stations in the network is denoted as N (i.e., $N = |X|$). The AIFS of station i is denoted as $\text{AIFS}_i = \text{DIFS} + \alpha_i \sigma$, where σ is the slot-time and α_i represents the number of additional slot-times that station i should differ. The notation $W_{l,i}$ represents the contention window size at the l -th backoff stage of station i and R is the maximum retry limit.

2.1 The Markov Chain Model

The Markov chain M_1 used in this paper is shown in Fig. 2. The states in M_1 are defined as $\{s(t), b(t), a(t)\}$, where $s(t)$ represents the backoff stage that is processed according to the binary exponential rules, while $b(t)$ is the stochastic process representing the backoff counter decremented at the end of every idle time-slot. If the channel is idle, then a station decrements its backoff counter (i.e., $b(t)$) by 1. When the backoff counter reaches zero, a station transmits. If the transmission encounters a collision with probability p_i , the backoff process proceeds to the next backoff stage (i.e., increased $s(t)$). In addition, $a(t)$ is introduced to model the influences of AIFS differences. In Fig. 2, the states with $\alpha_i \neq 0$ are introduced to model the awaiting counter based on the AIFS value of AC[i] (or equivalently, station i). Different ACs (stations) can have different values of α_i , and thus, corresponds to the additional awaiting time-slots before the actual backoff countdown takes place. When $\alpha_i = 0$, the Markov chain M_1 reduces to the seminal model presented in [14].

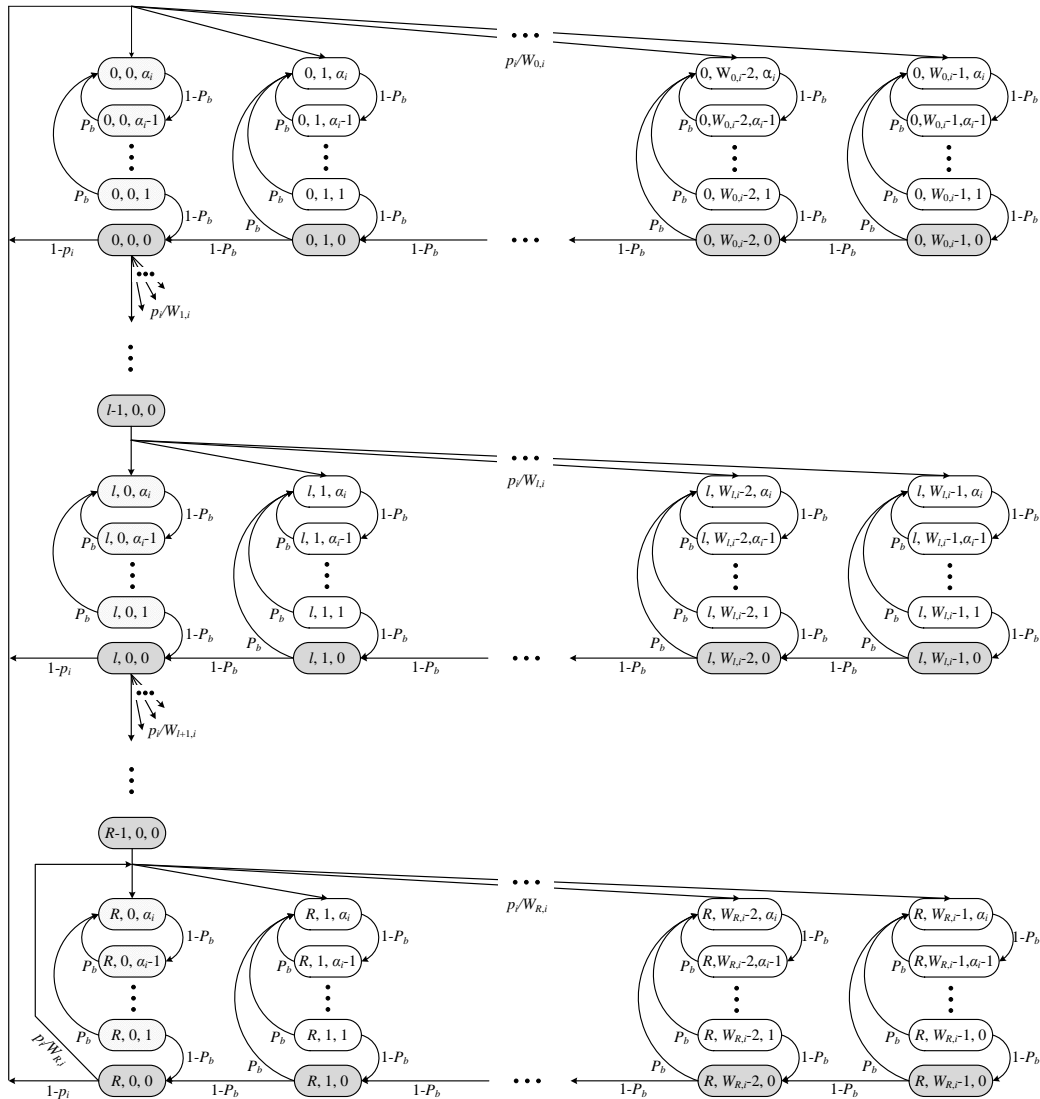


Fig. 2. Markov chain model for the backoff procedures (M_1).

The steady-state probability of M_1 in **Fig. 2** is $b_{l,m,n} = \lim_{t \rightarrow \infty} Pr\{s(t) = l, b(t) = m, a(t) = n\}$, $l \in [0, R]$, $m \in [0, W_{l,i} - 1]$, and $n \in [0, \alpha_i]$. The channel busy probability seen by any station in the network is denoted as P_b and can be obtained as follows.

$$P_b = 1 - \prod_{i \in X} (1 - \tau_i) \quad (1)$$

As mentioned earlier, the model relies on the unified view of the channel over all stations in the network, compared to other models in [2-14], where the channel states (busy or idle) seen by each station (AC) are individually computed. This approach, along with the Markov chain M_1 in **Fig. 2** where the AIFS countdowns are incorporated, significantly simplifies the analysis.

To compute the probability that station i will attempt to transmit (τ_i), the relationships between transmission stages, backoff states, and AIFS awaiting states can be represented as follows. From the Markov M_1 in **Fig. 2**, the following relations are obvious.

$$b_{l,0,0} = p_i^l \cdot b_{0,0,0}, \quad 0 < l < R \quad (2)$$

$$b_{R,0,0} = \frac{p_i^R}{1 - p_i} \cdot b_{0,0,0} \quad (3)$$

Considering the situation where $l = 0, \alpha_i = 0$, and $l = 0, \alpha_i = 1$, the following relations can be easily derived based on the balance conditions of the Markov chain M_1 .

$$b_{0,m,0} = (1 - P_b) \{b_{0,m,1} + b_{0,m+1,0}\}, \quad m \in [1, W_{0,i} - 1] \quad (4)$$

$$b_{0,W_0-1,0} = (1 - P_b) b_{0,W_0-1,0} \quad (5)$$

$$b_{0,0,1} = \frac{1 - p_i}{W_{0,i} (1 - P_b)} \sum_{i=0}^R b_{i,0,0} \quad (6)$$

$$b_{0,m,1} = \frac{1 - p_i}{W_{0,i} (1 - P_b)} \sum_{i=0}^R b_{i,0,0} + \frac{P_b}{1 - P_b} b_{0,n,0}, \quad m \in [1, W_{0,i} - 1] \quad (7)$$

Inserting (7) into (4) and (5), the probabilities of states with $l = 0, m \in [1, W_{l,i} - 1]$, and $n = 0$ can be expressed as in (8). The probability of states with other l values (i.e., when $0 < l < R$, and when $l = R$) can be obtained by a similar approach, and are shown in (9) and (10), respectively.

$$b_{0,m,0} = \left(\frac{W_{0,i} - m}{W_{0,i}} \right) \left(\frac{1 - p_i}{1 - P_b} \right) \cdot \sum_{i=0}^R b_{i,0,0}, \quad m \in [1, W_{0,i} - 1] \quad (8)$$

$$b_{l,m,0} = \left(\frac{W_{l,i} - m}{W_{l,i}} \right) \left(\frac{p_i}{1 - P_b} \right) \cdot b_{l-1,0,0}, \quad m \in [1, W_{l,i} - 1] \quad (9)$$

$$b_{0,m,0} = \left(\frac{W_{R,i} - m}{W_{R,i}} \right) \left(\frac{p_i}{1 - P_b} \right) \cdot \{b_{R-1,m,0} + b_{R,m,0}\}, \quad m \in [1, W_{R,i} - 1] \quad (10)$$

Using relations (2) and (3), the overall probabilities of state with $l \in [0, R]$, $m \in [1, W_{l,i} - 1]$, and $n = 0$ can be generalized as in (11) below. Therefore, based on (2), (3), and (11), the probability of states with a shaded circle in **Fig. 2** are now expressed in terms of $b_{l,0,0}$.

$$b_{l,m,0} = \left(\frac{W_{l,i} - m}{W_{l,i}} \right) \left(\frac{1}{1 - P_b} \right) \cdot b_{l,0,0}, \quad l \in [0, R], \quad m \in [1, W_{R,i} - 1] \quad (11)$$

For the states with $l \in [0, R]$, $m = 0$, and $n = [1, \alpha_i]$, $b_{l,0,n} = (1 - P_b)^{\alpha_i - n} b_{l,0,\alpha_i}$ for $n \in [1, \alpha_i]$. Using the rules of geometric series, the following can be obtained.

$$\sum_{n=1}^{\alpha_i - 1} b_{l,0,n} = (1 - P_b)^{\alpha_i - 1} \cdot b_{l,0,\alpha_i} \sum_{n=1}^{\alpha_i - 1} \left(\frac{1}{1 - P_b} \right)^n = \left(\frac{1}{P_b} \right) \left\{ (1 - P_b) - (1 - P_b)^{\alpha_i} \right\} \cdot b_{l,0,\alpha_i} \quad (12)$$

Using (12), the probability of states with $l \in [0, R]$, $m = 0$, and $n = [1, \alpha_i]$ (dashed circles in Fig. 2) can be derived as in (13).

$$b_{l,0,n} = \frac{1}{W_{l,i} (1 - P_b)^n} b_{l,0,0}, \quad l \in [0, R], \quad n \in [1, \alpha_i] \quad (13)$$

In a similar way, the probability of states with $l \in [0, R]$, $m \in [1, W_{l,i} - 1]$, and $n = [1, \alpha_i]$ (white circles in Fig. 2) can be obtained as follows.

$$b_{l,m,n} = \frac{1}{W_{l,i} (1 - P_b)^n} b_{l,0,0} + \frac{P_b}{(1 - P_b)^n} b_{l,m,0}, \quad l \in [0, R], \quad m \in [1, W_{l,i} - 1], \quad n \in [1, \alpha_i] \quad (14)$$

Based on (2), (3), (11), (13), and (14) being expressed as a function of $b_{l,0,0}$ (i.e., $b_{0,0,0}$ since $b_{l,0,0} = p^l b_{0,0,0}$ for $0 < l < R$ and $b_{R,0,0} = p^R b_{0,0,0} / (1 - p)$), the steady-state probability of all states in the Markov chain M_1 are established. Applying the normalization condition, the following expression for $b_{0,0,0}$ can be obtained.

$$\begin{aligned} \sum_{l=0}^R \sum_{m=0}^{W_{l,i}-1} \sum_{n=0}^{\alpha_i} b_{l,m,n} &= \sum_{l=0}^R \sum_{m=0}^{W_{l,i}-1} \left[b_{l,m,0} + \sum_{n=1}^{\alpha_i} b_{l,m,n} \right] = \sum_{l=0}^R \left[b_{l,0,0} + \sum_{m=1}^{W_{l,i}-1} b_{l,m,0} \right] + \sum_{l=0}^R \left[\sum_{n=1}^{\alpha_i} b_{l,0,n} + \sum_{m=1}^{W_{l,i}-1} \sum_{n=1}^{\alpha_i} b_{l,m,n} \right] \\ &= \left[1 + \frac{1}{P_b (1 - P_b)^{\alpha_i}} - \frac{1}{P_b} \right] \sum_{l=0}^R b_{l,0,0} + \frac{1}{(1 - P_b)^{\alpha_i + 1}} \sum_{l=0}^R \left(\frac{W_{l,i} - 1}{2} \right) b_{l,0,0} \\ &= \frac{(1 - 2p_i)[2(1 - P_b)(1 - (1 - P_b)^{\alpha_i + 1}) + P_b(W_{0,i} - 1)] + p_i P_b W_{0,i} (1 - (2p_i)^R)}{2P_b(1 - P_b)^{\alpha_i + 1}(1 - 2p_i)(1 - p_i)} b_{0,0,0} = 1 \end{aligned} \quad (15)$$

Since a transmission occurs when the backoff counter reaches zero, the transmission probability of station i (τ_i) can be obtained as in (16), based on (15). Therefore, the throughput of EDCA stations can be expressed as a system of N nonlinear equations on the τ_i 's, which can be solved by using numerical techniques together with (17).

$$\tau_i = \sum_{l=0}^R b_{l,0,0} = \frac{b_{0,0,0}}{1 - p_i} = \frac{2P_b(1 - P_b)^{\alpha_i + 1}(1 - 2p_i)}{(1 - 2p_i)[2(1 - P_b)(1 - (1 - P_b)^{\alpha_i + 1}) + P_b(W_{0,i} - 1)] + p_i P_b W_{0,i} (1 - (2p_i)^R)} \quad (16)$$

$$P_i = 1 - \prod_{j \in X \setminus i} (1 - \tau_j) \quad (17)$$

2.2 Throughput Expressions

The normalized throughput can be defined as the amount of average information transmitted during the transmission period. Based on this definition, the normalized throughput of station i can be expressed as follows.

$$S_i = \frac{P_s(i)D_i}{P_s T_s(i) + P_c T_c(i) + P_e \sigma} \quad (18)$$

In (18), D_i is the average frame payload size of station i and σ is the slot-time. $P_s(i)$ is the probability of successful transmission of station i and P_s is the overall successful transmission probability (i.e., probability that a randomly chosen slot-time contains a successful transmission). In addition, P_e and P_c is the probability that a slot-time is empty (i.e., idle) and the probability that a slot-time contains a collision, respectively. The expressions for $P_s(i)$, P_s , P_c , and P_e are shown below.

$$P_s(i) = \tau_i \prod_{j \in X \setminus i} (1 - \tau_j), \quad P_s = \sum_{i \in X} P_s(i) \quad (19)$$

$$P_e = \prod_{i \in X} (1 - \tau_i) = 1 - P_b \quad (20)$$

$$P_c = \sum_{i \in X} \tau_i \left(1 - \prod_{j \in X \setminus i} (1 - \tau_j) \right) = 1 - P_s - P_e \quad (21)$$

The corresponding successful transmission and collision time of station i (i.e., $T_s(i)$ and $T_c(i)$) are shown below for the basic access mode,

$$T_s(i) = T_{\text{PLCP}} + (H + D_i)/C + \text{SIFS} + \delta + \text{ACK} + \text{AIFS}_i + \delta \quad (22)$$

$$T_c(i) = T_{\text{PLCP}} + (H + D_i)/C + \text{AIFS}_i + \delta \quad (23)$$

where T_{PLCP} is the PLCP (Physical Layer Convergence Protocol) header duration, H is the MAC header size, and δ is the propagation delay. For the case of *request-to-send/clear-to-send* (RTS/CTS) mode, these times can be expressed as follows.

$$T_s(i) = \text{RTS} + \text{SIFS} + \delta + \text{CTS} + \text{SIFS} + \delta + T_{\text{PLCP}} + (H + D_i)/C + \text{SIFS} + \delta + \text{ACK} + \text{AIFS}_i + \delta \quad (24)$$

$$T_c(i) = \text{RTS} + \text{AIFS}_i + \delta \quad (25)$$

To validate the accuracy of the model presented in the previous subsection, the results are compared with the model proposed in [2] and NS-2 simulation results in Fig. 3 where the throughput performance of two ACs are plotted (number of stations per AC is fixed to 2 and 10, respectively). In addition, the results of 4 ACs are compared based on NS-2 simulations results

in Fig. 4. Other system parameters are the same as Table 1 of [2], except the payload length was set to 1000 bytes. From Fig. 3, it can be observed that the model provides more accurate results than [2]. In addition, it is confirmed in Fig. 4 that the model can track more than two ACs at the same time with reasonable accuracy at a significantly reduced computational complexity (since it does not rely on contention-zones).

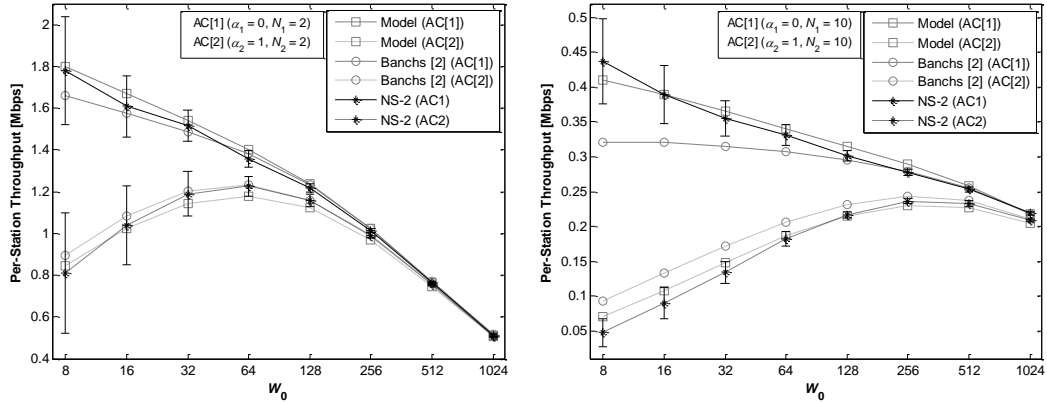


Fig. 3. Results of two ACs (2 and 10 stations per AC, respectively)

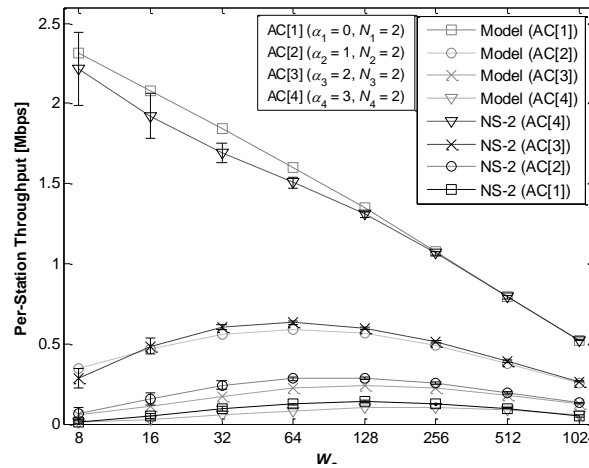


Fig. 4. Results of four ACs (2 stations per AC)

2.3 Optimization Statements

Since the objective is to maximize the throughput of each station, the problem can be formulated as a multi-objective optimization problem as shown in (26), where $W_{0,i}$ and C_i represents the minimum CW size and the capacity of station i , respectively. The objective functions (i.e., $S_i(\mathbf{W}_0)$) represents the throughput of each station obtained from (18), which are in conflict of interest with each other since an effort to increase the performance of one objective function will commonly result in degradations of the other objectives.

$$\begin{aligned}
 &\text{Maximize } \mathbf{S}(\mathbf{W}_0) = [S_1(\mathbf{W}_0), S_2(\mathbf{W}_0), \dots, S_N(\mathbf{W}_0)]^T \\
 &\text{Subject to } S_i(\mathbf{W}_0) \geq 0, \forall i \in X \\
 &\quad S_i(\mathbf{W}_0) \leq C_i, \forall i \in X \\
 &\quad \mathbf{W}_0 = [W_{0,1}, W_{0,2}, \dots, W_{0,N}]^T, W_{0,i} \geq 0, \forall i \in X
 \end{aligned} \tag{26}$$

Fig. 5 represents the Pareto optimal front of an EDCA WLAN with 2 ACs (i.e., AC[1] and AC[2]) when $N_1 = N_2 = 5$ and $\alpha_1 = \alpha_2 = 0$. It can be observed that the throughput achieved by the stations of different ACs are in conflict with each other, and as a result, increasing the allocated ratio of one AC results in degradation in the other AC.

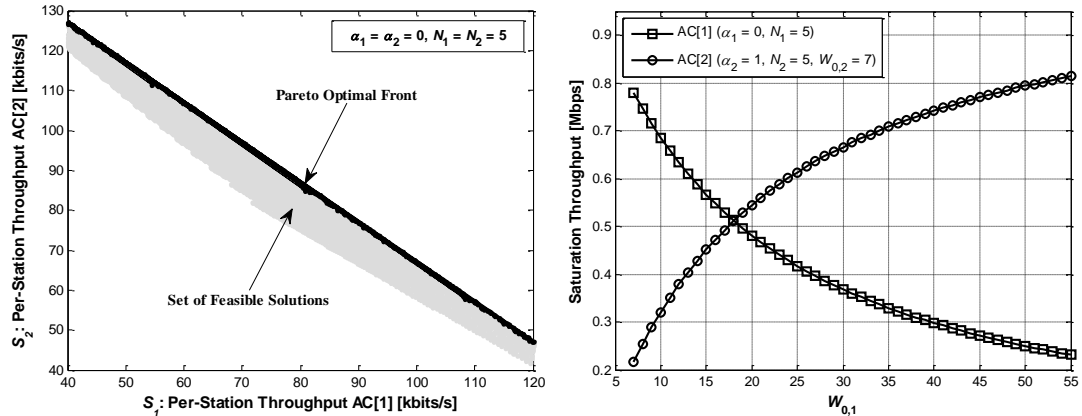


Fig. 5. Pareto optimal front for problem in (26) and saturation throughput of AC[1] and AC[2].

As stated in the previous section, packet transmissions of stations of one AC are cross-related with that of the stations of other ACs. The reason for this phenomenon is based upon the fact that transmissions are governed by the random backoff procedures and differences in QoS parameters. Although the ACs are separated with different priorities, we cannot predict the exact order of sequence of transmissions, since the transmission times of both ACs show random behavior. This can be verified from **Fig. 5**, where $W_{0,2}$ is set to 7, $W_{0,1}$ varies from 7 to 55, $\alpha_1 = 0$, $\alpha_2 = 1$, and $N_1 = N_2 = 5$. **Fig. 5** represents the saturation throughput of AC[1] and AC[2]. As can be seen from **Fig. 5**, since the two ACs are closely correlated with each other, if one AC tries to increase its throughput by lowering its CW value, the stations of the other ACs will suffer degradation in throughput performance.

Since the nature of the backoff process creates a conflict, and considering the interactive behavior of different stations of different ACs, the objective of maximizing per station throughput as well as the overall system throughput cannot be easily modeled into a single objective optimization problem, but is better to be dealt with in a multi-objective Pareto optimization form. The analytical derivations of the throughput model in the previous section includes these cross effects of conflicting probabilities due to different system parameters (CWs and AIFSs), where the proposed algorithm introduced in the following sections provide a Pareto optimized system throughput performance.

A more precise problem statement compared to (26) is provided in (27), where it is assumed that the priority of the stations are ordered in an ascending order (i.e., $P_i > P_j$, if $i < j$ for all $i, j \in X$). Therefore, station 1 is the highest priority station and the required relative throughput proportion of station i (R_i) is normalized based on S_1 (i.e., $R_i = S_i/S_1$ and $R_1 = 1$).

$$\begin{aligned}
 \text{Maximize } \mathbf{S}(\mathbf{W}_0) &= \begin{bmatrix} S_1(\mathbf{W}_0) = \{S_1 | S_1 \leq R_1 S_1\} \\ S_2(\mathbf{W}_0) = \{S_2 | S_1 \leq R_1 S_1, S_2 \leq R_2 S_1\} \\ \vdots \\ S_N(\mathbf{W}_0) = \{S_N | S_1 \leq R_1 S_1, S_2 \leq R_2 S_1, \dots, S_N \leq R_N S_N\} \end{bmatrix} \\
 \text{Subject to } 0 \leq S_i(\mathbf{W}_0) &\leq C_i, \quad \forall i \in X, \\
 R_i &= S_i / S_1, \quad \forall i \in X \\
 \mathbf{W}_0 &= [W_{0,1}, W_{0,2}, \dots, W_{0,N}]^T, \quad W_{0,i} \geq 0, \quad \forall i \in X
 \end{aligned} \tag{27}$$

In (27), it can be seen that the throughput S_1 is upper-bounded by the desired ratio R_1 . In addition, the throughput S_2 is constrained by the higher priority throughput allocation (S_1) and by the desired ratio of its own (R_2). The same pattern of upper-bounds and throughput allocation constraints apply to the lower priority stations as well.

3. QoS Provisioning Parameter Control

3.1 Finding a Near-Optimal Configuration

A simple and straightforward way to find the optimal solution would be to perform a brute force search for all of parameter configurations. However, finding the optimal configuration in this fashion would definitely be impractical. To reduce the computational complexity, the initial starting points have to be programmed to begin at a near-optimal point before applying the proposed algorithm described in the following subsection.

Assuming $T_S(i) = T_S$, $T_C(i) = T_C$, $D_i = D$ for $\forall i \in X$, and using (19)~(21), the throughput expression in (18) can be rewritten as follows, where $y_i = \tau_i / (1 - \tau_i)$.

$$S_i = \frac{y_i (D / T_C)}{(\sigma / T_C - 1) + (T_S / T_C - 1) \sum_{j \in X} y_j + \prod_{k \in X} (1 + y_k)} \tag{28}$$

When $\tau_i \ll 1$, then $1 - \tau_i \approx 1$ and $\tau_i \approx R_i \tau_1$, therefore resulting in $y_i \approx R_i \tau_1$. The initial starting point will be selected such that it maximizes $S_T = \sum_{i \in X} S_i$, as shown below.

$$\begin{aligned}
 S_T &= \sum_{i \in X} S_i = \sum_{i \in X} \frac{R_i \tau_1 (D / T_C)}{(\sigma / T_C - 1) + (T_S / T_C - 1) \sum_{j \in X} R_j \tau_1 + \prod_{k \in X} (1 + R_k \tau_1)} \\
 &= \sum_{i \in X} \frac{R_i (D / T_C)}{[(\sigma / T_C - 1) + \prod_{k \in X} (1 + R_k \tau_1)] / \tau_1 + (T_S / T_C - 1) \sum_{j \in X} R_j \tau_1}
 \end{aligned} \tag{29}$$

From (29), it is obvious that maximizing S_T is equivalent to minimizing the function $Z(\tau_1) = [(\sigma / T_C - 1) + \prod_{k \in X} (1 + R_k \tau_1)] / \tau_1$. By denoting $f(\tau_1) = \prod_{k \in X} (1 + R_k \tau_1)$, $f(\tau_1)$ can be approximated as follows using Taylor series expansion.

$$f(\tau_1) = \prod_{k \in X} (1 + R_k \tau_1) \approx f(0) + f'(0) \tau_1 + f''(0) \tau_1^2 \tag{30}$$

Where $f(0) = 1, f'(0)$ and $f''(0)$ can be written as follows.

$$f'(0) = \sum_{i \in X} R_i = \sum_{i=1}^N R_i \tag{31}$$

$$f''(0) = \frac{1}{2} \left[\left(\sum_{i=1}^N R_i \right)^2 + \sum_{i=1}^N R_i^2 \right]. \tag{32}$$

Therefore, $Z(\tau_1) = [(\sigma/T_c - 1) + f(0) + f'(0)\tau_1 + f''(0)\tau_1^2]/\tau_1$. Differentiating $Z(\tau_1)$ with respect to τ_1 and by setting it to zero, the following optimal point for τ_i and p_i can be obtained.

$$\tau_i^* = \begin{cases} \left(\frac{T_c}{2\sigma} \left[\left(\sum_{i=1}^N R_i \right)^2 + \sum_{i=1}^N R_i^2 \right] \right)^{-1/2} & \text{if } i = 1 \\ \frac{R_i \tau_1^*}{1 - \tau_1^* (1 - R_i)} & \text{otherwise} \end{cases} \tag{33}$$

$$p_i^* = 1 - \sum_{j \in X^i} (1 - \tau_j^*) \tag{34}$$

The initial CW configuration can be represented as follows based on (16), (33), and (34), where $y_i^* = (1 - \tau_1^*)/\tau_1^*$.

$$W_{0,i}^* = \frac{(1 - 2p_i^*) [2(1 - P_b)^{\alpha_i + 1} (1 + y_i^* P_b) + 3P_b - 2]}{P_b [1 - p_i^* (1 + (2p_i^*)^R)]} \tag{35}$$

The results obtained from (35) will be used as an initial starting point of the proposed algorithm in the following subsection. The approximated $W_{0,i}^*$ are shown in Fig. 5 for various relative throughput ratios allocated (2 ACs only for spatial limitations).

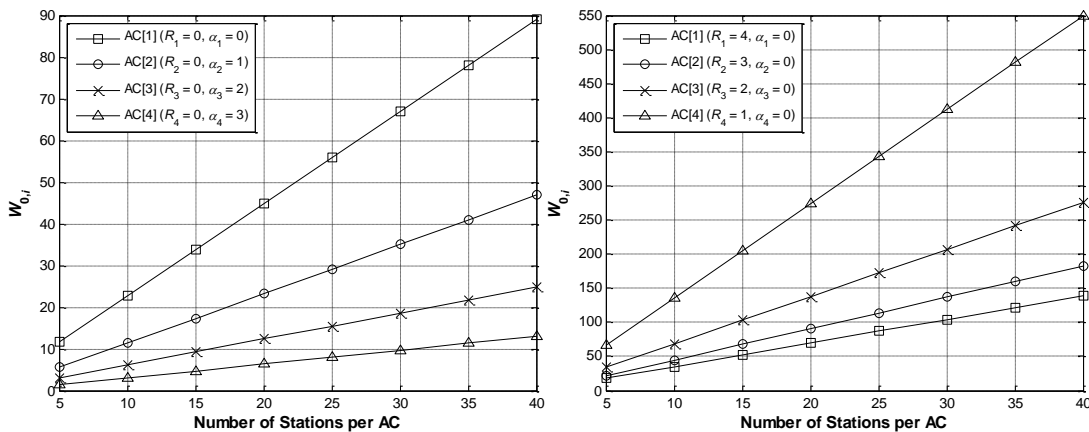


Fig. 6. Approximated CW for various relative throughput ratios and AIFS differentiation.

3.2 Parameter Control Algorithm

The proposed QoS provisioning parameter control algorithm is based on two input variables: the desired relative throughput ratio of station i (R_i) and the number of competing stations (N) in the network. For the output, it provides the minimum contention window size values for all stations in the network, which eventually enables the stations to operate in Pareto optimal system configurations. The pseudo code of the proposed algorithm is provided in **Table 1**, and explanations based on the line numbers are presented below. In **Table 1**, $\mathbf{R} = \{R_1, \dots, R_N\}$ is a n -dimensional vector whose elements are the desired relative throughput ratios. In addition, $\mathbf{W}^* = \{W_1^*, W_2^*, \dots, W_N^*\}$ is the candidate CW vector and $\mathbf{P}^* = \{P_1^*, P_2^*, \dots, P_N^*\}$ is the set of candidate Pareto optimal configurations.

Table 1. QoS Provisioning Parameter Control Algorithm

Parameter Control Algorithm	
1:	Start
2:	For every UPDATETIME do
3:	Initialize {
4:	Identify $\mathbf{R} = \{R_1, \dots, R_N\}$ and N
5:	$\mathbf{W}^* = \{W_1^*, W_2^*, \dots, W_N^*\} \leftarrow \emptyset$
6:	$\mathbf{P}^* = \{P_1^*, P_2^*, \dots, P_N^*\} \leftarrow \emptyset$ }
7:	Creating candidate \mathbf{W}^*
8:	for $i \in X$ {
9:	W_i^* based on (35)
11:	$m_i = (1 - \epsilon r_i)W_i^*$ to $(1 + \epsilon r_i)W_i^*$ }
12:	$\mathbf{W}^* \leftarrow \mathbf{W}^* \cup \{(m_1, \dots, m_m)\}$
13:	Generating Pareto Optimal Solution
14:	$\mathbf{P}^* \leftarrow \mathbf{P}^* \cup \mathbf{W}^*$
15:	for $x \in \mathbf{W}^*$ {
16:	if $F_i(x) \leq F_i(p^*), \forall p^* \in \mathbf{P}^*, \forall i \in X$ // case A
17:	else if $F_i(x) > F_i(p^*), \exists p^* \in \mathbf{P}^*, \forall i \in X$ // case B
18:	for $p^* \in \mathbf{P}^*$ {
19:	if $F_i(x) > F_i(p^*), \forall i \in X$
21:	$\mathbf{P}^* \leftarrow \mathbf{P}^* - \{p^*\}$ }
23:	else $\mathbf{P}^* \leftarrow \mathbf{P}^* \cup \{x\}$ } // case C
24:	return \mathbf{P}^*

- **Lines 1~2:** Reconfigure \mathbf{W}^* every UPDATETIME. This is operated by the AP every beacon interval. Then, the newly obtained configuration is distributed to stations.
- **Lines 3~6:** The AP detects the number of stations that are involved in transmission competition (N) and the desired resource allocation ratios of stations (\mathbf{R}). In addition, create candidate CW set (\mathbf{W}^*) and the Pareto solution set (\mathbf{P}^*), which is a set of the non-dominating values.
- **Lines 7~12:** Update \mathbf{W}^* and check the domination/non-domination properties of each elements. The approximated initial \mathbf{W}^* is obtained from (35). The approximation results in a near optimal \mathbf{W}^* , where ϵr_i is the user-defined expected error range of station i (set to 10% in the simulations).
- **Lines 13~23:** Determine if the point is a non-dominated point or not (Pareto optimality).

The objects of comparison include all elements of the candidate W^* set obtained earlier. The candidates are classified under one of the following three solution cases **A**, **B**, or **C**. In case **A**, where a candidate solution x (an element of the candidate W^* set) is dominated by a candidate solution, then the set of existing Pareto solutions P^* are not changed. For case **B**, if a candidate solution x dominates at least one other candidate solution, then the dominated solution(s) are deleted from the Pareto solution set, and the new solution x is added to the set of Pareto solutions P^* . For case **C**, if x does not dominate any of the existing candidates, then x is added as a new Pareto solution P^* .

- **Line 24:** The CW of the Pareto optimal front P^* are distributed to stations and applied until the next UPDATETIME.

The proposed algorithm is different from [6] and [7] as it configures the optimal CW that results in a maximum saturation throughput by using the prediction method described in the previous section and then additionally applying the proposed algorithm based on a local-value adjustment method to the parameter settings such that similar configurations of pre-identified Pareto optimal points can be checked for domination/non-domination in order to efficiently obtain other non-dominated values near that point. In the following section, a performance comparison between the proposed algorithm and the scheme of [6] is presented.

4. Simulation Results

Fig. 7 and **Fig. 8** presents the results obtained from extensive simulations conducted on Network Simulator 2 (NS-2) [15]. The simulation results presented in **Fig. 7** were conducted with two ACs (i.e., AC[1] and AC[2]), where $\alpha_1 = \alpha_2 = 0$, $N_1 = N_2 = 5$, and one packet transmission per TXOP. The channel capacity was set to 1 Mbps and the payload size was set to 1000 bytes per packet. For the model in [6], the default CW of the highest priority AC (i.e., AC[1]) was set to 7, same as in the standards, and the window size of the lower priority AC (i.e., AC[2]) was set according to the algorithm described in [6]. For the proposed model, the window sizes were configured using the QoS provisioning parameter control algorithm presented in section 3.2. To obtain **Fig. 8**, for throughput ratio 6:4, $W_{0,3}$ was set to 26 and $W_{0,2}$ was set to 38. For throughput ratio 7:3, $W_{0,3} = 23$ and $W_{0,2} = 51$ was applied, and for ratio 8:2, $W_{0,3} = 20$ and $W_{0,2} = 72$ was applied. Finally, for throughput ratio 9:1, $W_{0,3}$ was set to 17 and $W_{0,2}$ was set to 140. All other system parameters were configured according to [10].

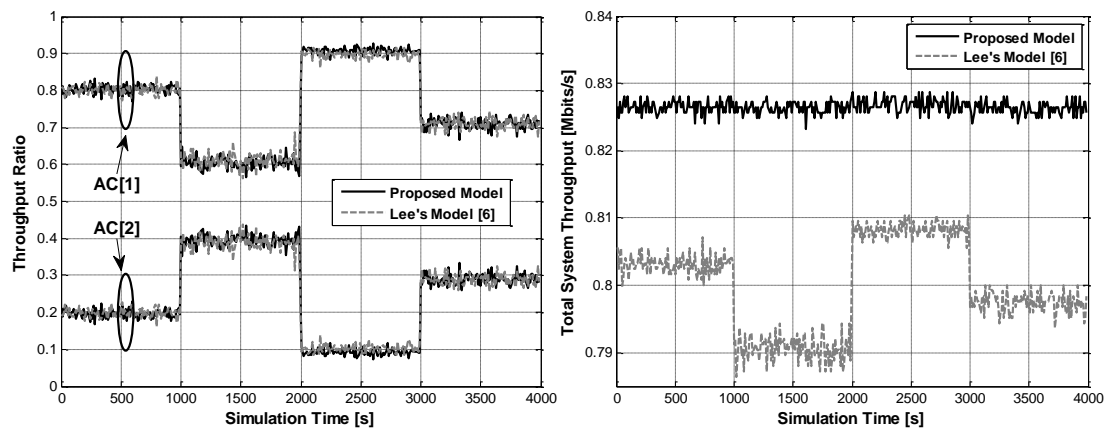


Fig. 7. Throughput allocation control and the total system throughput performance

In Fig. 7, the desired throughput ratio was changed from 8:2 to 6:4, 9:2, and 7:3. In Fig. 7, it can be seen that both the proposed algorithm and the algorithm proposed in [6] are capable of controlling the ratio of resources allocated. However, the total system throughput fluctuates when there is a change in the desired throughput ratio when using the algorithm of [6]. In general, the algorithm of [6] cannot maximize the channel utilization and therefore cannot provide an optimized performance. In contrast, the proposed algorithm maintains almost a constant total system throughput (about 0.827 Mbits/s on average) in every situation. In other words, the proposed algorithm is able to fully utilize the channel in near-Pareto optimized network configurations. This is possible because the proposed algorithm approximates a Pareto optimal system performance by selecting control parameters that form the Pareto optimal front. This result is also confirmed by the per-class saturation throughput performance presented in Fig. 8, which was obtained by extending the results of Fig. 7 by varying the number of stations. The results confirm that the proposed algorithm improves the overall system performance of WLANs regardless of the number of stations and the required (desired) throughput ratios.

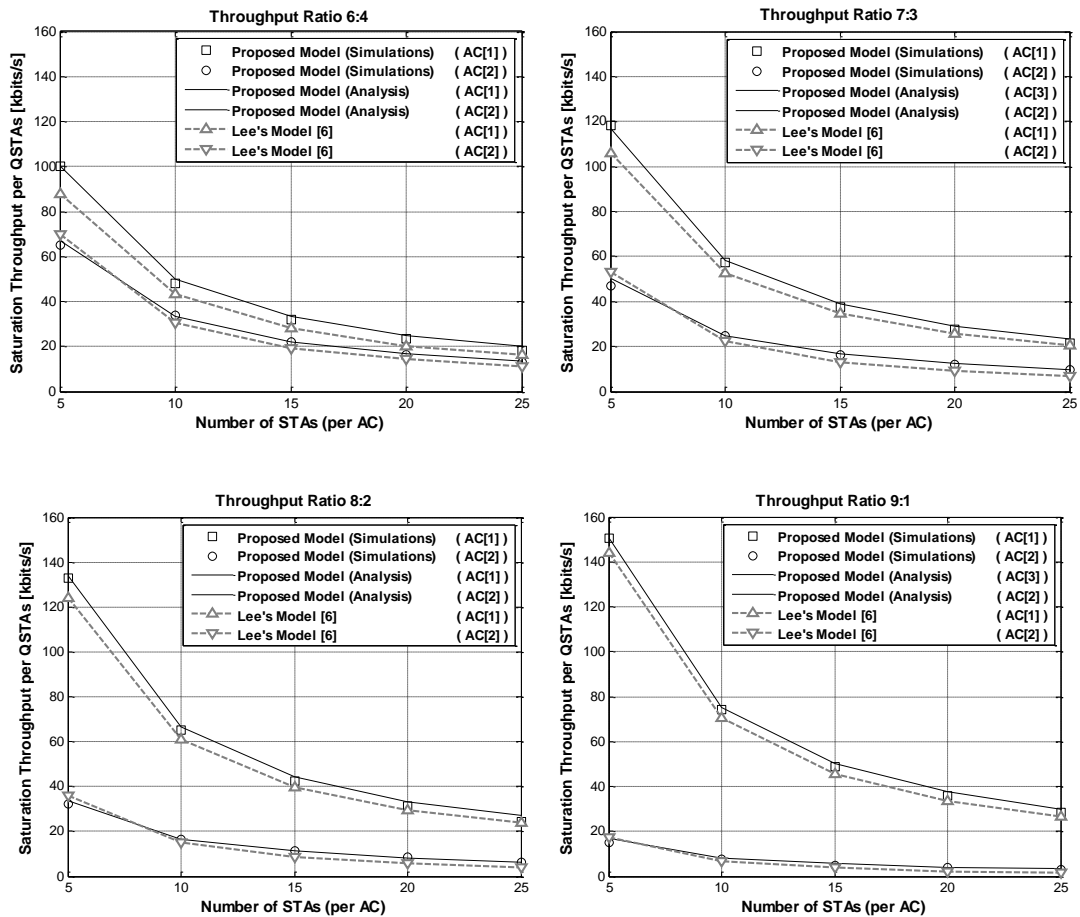


Fig. 8. Per-Class throughput performance for various allocation ratio.

5. Conclusion

In this paper, a simple and accurate model to analyze the saturation throughput of EDCA networks is provided. Based on this, a QoS provisioning parameter control algorithm is proposed. The proposed algorithm can provide an enhanced system throughput performance, while maintaining the desired proportion of per-station resource allocation. Furthermore, the proposed algorithm can provide user controllability to stations that are participating in the network. Although the proposed scheme requires additional computational overhead, the simulation results confirm the efficiency of the proposed algorithm and demonstrate that the proposed scheme significantly outperforms the default parameter settings and also outperforms the other EDCA control methods that have been discussed in the introduction.

For future works, the model introduced in section II should be extended so that it can provide adaptive control not only for throughput, but also for the delay performance. Based on this, the parameter control scheme should also be extended, considering both the throughput and delay requirements of each AC. Since there are strict time requirements for some ACs, the extensions mentioned above will make the proposed scheme more practical and feasible.

References

- [1] "IEEE 802.11e, Part 11: Wireless Medium Access Control (MAC) and Physical Layer (PHY) Specifications: Medium Access Control (MAC) Quality of Service Enhancements," *IEEE Std. 802.11e-2005*, Nov. 2005. [Article \(CrossRef Link\)](#)
- [2] A. Banchs and L. Vullero, "Throughput analysis and optimal configuration of 802.11e EDCA," *Computer Networks*, vol. 50, no. 11, pp. 1749-1768, August, 2006. [Article \(CrossRef Link\)](#)
- [3] P. Patras, A. Banchs, and P. Serrano, "A control theoretic approach for throughput optimization in IEEE 802.11e EDCA WLANs," *Mobile Networks and Applications*, vol. 14, no. 6, pp. 697-708, December, 2009. [Article \(CrossRef Link\)](#)
- [4] P. Serrano, A. Banchs, P. Patras, and A. Azcorra, "Optimal configuration of 802.11e EDCA for real-time and data traffic," *IEEE Transactions on Vehicular Technology*, vol. 59, no. 5, pp. 2511-2528, June, 2010. [Article \(CrossRef Link\)](#)
- [5] J. Y. Lee and H. S. Lee, "A performance analysis model for IEEE 802.11e EDCA under saturation condition," *IEEE Transactions on Communications*, vol. 57, no. 1, pp. 56-63, January, 2009. [Article \(CrossRef Link\)](#)
- [6] J. Y. Lee, H. S. Lee, and J. S. Ma, "Model-based QoS parameter control for IEEE 802.11e EDCA," *IEEE Transactions on Communications*, vol. 57, no. 7, pp. 1914-1918, July, 2009. [Article \(CrossRef Link\)](#)
- [7] Z. Fan, "Throughput and QoS optimization for EDCA-based IEEE 802.11 WLANs," *Wireless Personal Communications*, vol. 43, no. 4, pp. 1279-1290, December, 2007. [Article \(CrossRef Link\)](#)
- [8] G. Bianchi, I. Tinnirello, and L. Scalia, "Understanding 802.11e contention-based prioritization mechanism and their coexistence with legacy 802.11 stations," *IEEE Network*, vol. 19, no. 4, pp. 28-34, July, 2005. [Article \(CrossRef Link\)](#)
- [9] I. Inan, F. Keceli, and E. Ayanoglu, "Analysis of the 802.11e enhanced distributed channel access function," *IEEE Transactions on Communications*, vol. 57, no. 6, pp. 1753-1764, June, 2009. [Article \(CrossRef Link\)](#)
- [10] J. W. Robinson and T. S. Randhawa, "Saturation throughput analysis of IEEE 802.11e enhanced distributed coordination function," *IEEE Journal on Selected Areas in Communications*, vol. 22, no. 5, pp. 917-928, June, 2004. [Article \(CrossRef Link\)](#)
- [11] Y. P. Fallah, S. El-Housseini, and H. Alnuweiri, "A generalized saturation throughput analysis for IEEE 802.11e contention-based MAC," *Wireless Personal Communications*, vol. 47, no. 2, pp. 235-245, October, 2008. [Article \(CrossRef Link\)](#)

- [12] F. Peng, B. Peng, and D. Qian, "Performance analysis of IEEE 802.11e enhanced distributed channel access," *IET Communications*, vol. 4, no. 6, pp. 728-738, April, 2010. [Article \(CrossRef Link\)](#)
- [13] M. Garreto, T. Salonidis, and E. W. Knightly, "Modeling per-flow throughput and capturing starvation in CSMA multi-hop wireless networks," *IEEE/ACM Transactions on Networking*, vol. 16, no. 4, pp. 864-877, August, 2008. [Article \(CrossRef Link\)](#)
- [14] G. Bianchi, "Performance analysis of the IEEE 802.11 distributed coordination function," *IEEE Journal on Selected Areas in Communications*, vol. 18, no. 3, pp. 535-547, March, 2000. [Article \(CrossRef Link\)](#)
- [15] The Network Simulator, NS2. [Article \(CrossRef Link\)](#)



Minseok Kim received his B.S. and Ph.D. degrees from the School of Electrical and Electronic Engineering, Yonsei University, Seoul, Republic of Korea, in 2009 and 2014, respectively. Since 2014, he has been with Samsung Electronics Co. Ltd., where he is focusing on software engineering for wearable devices and internet-of-things (IOT) environments. His research focuses on mobile and ad hoc wireless networks, device-to-device (D2D) communications, scheduling, MAC protocols, software engineering, and vehicular communications.



Wui Hwan Oh received his B.S. degree from the Department of Ceramic Engineering, Hanyang University, Seoul, Republic of Korea, in 2005. In 2011, he received his M.S. degree from the School of Electrical and Electronic Engineering, Yonsei University. Since 2005, he has been with Republic of Korea Army. His research focuses on future combat systems, military communications, common datalink, mobile ad-hoc network, and MAC protocols for wireless networks.



Jong-Moon Chung received B.S. and M.S. degrees from Yonsei University, and Ph.D. degree from the Pennsylvania State University. He has been a professor in the School of Electrical and Electronic Engineering, Yonsei University, since 2005. He served as an assistant professor in the Department of Electrical Engineering at the Pennsylvania State University, and has served as Director of OCLNB and ACSEL labs and served as a tenured associate professor at the Oklahoma State University. His research is in the area of smartphone design, network scheduler design, LTE/5G, IoT, M2M, Mobile-CDN, AR, CR, SDN, NFV, SDN, MANET, VANET, ITS, satellite communications, military communications, and broadband QoS networking. He is an Editor of the IEEE Trans. on Vehicular Technology and Co-Editor-in-Chief of the KSII TIS.



Bong Gyou Lee is a Professor at the Graduate School of Information and has served as a Director of the Communications Policy Research Center (CPRC) in Yonsei University since 2009. Dr. Lee received a B.A. from the Department of Economics at Yonsei University and M.S. and Ph.D. from Cornell University. During 2007 and 2008 he served as Commissioner of the Korea Communications Commission.



Myunghwan Seo received his B.S. degree in Information and Communication Engineering from Chungnam National University, Daejeon, Korea in 2002, and earned his M.S. and Ph.D. degrees in information and Communication Engineering from the Korea Advanced Institute of Science and Technology (KAIST), Daejeon, Korea in 2004 and 2009, respectively. Since 2009, he has been worked with Samsung Thales Col Ltd., where he is focusing on developing wireless communication protocols for military wireless communication systems. His research interests are mobile ad-hoc networks, wireless mesh networks, wireless MAC protocols, cognitive radio, and military wireless communications.



Jung-sik Kim received his B.S. and M.S. degrees in Computer Engineering, Kyungpook National University, Daegu, Korea, in 2005 and 2007, respectively. From 2007 to 2011, he worked as a researcher in the Electronics and Telecommunications Research Institute (ETRI), Daejeon, Korea. Since 2011, he has been with Samsung Thales Co. Ltd., where he is focusing on software engineering for military wireless communication systems. His research interests include mobile ad-hoc network, wireless sensor network, network synchronization, and military wireless communications.



Hyung-Weon Cho has been with Samsung Thales Co. Ltd. since 1997, where he is focusing on system engineering for tactical mobile communication systems, software defined radio and cognitive radio. He received Ph.D. degrees from the School of Electrical and Electronic Engineering, Yonsei University, Seoul, Republic of Korea, in 2012.